DOI: 10.1534/genetics.108.088948

# The T-Box Gene *tbx-2*, the Homeobox Gene *egl-5* and the Asymmetric Cell Division Gene *ham-1* Specify Neural Fate in the HSN/PHB Lineage

**Aakanksha Singhvi, C. Andrew Frank[1] and Gian Garriga[2]**

*Department of Molecular and Cell Biology, Helen Wills Neuroscience Institute, University of California, Berkeley, California 94720*

Manuscript received March 5, 2008
Accepted for publication April 5, 2008

ABSTRACT

Understanding how neurons adopt particular fates is a fundamental challenge in developmental neurobiology. To address this issue, we have been studying a *Caenorhabditis elegans* lineage that produces the HSN motor neuron and the PHB sensory neuron, sister cells produced by the HSN/PHB precursor. We have previously shown that the novel protein HAM-1 controls the asymmetric neuroblast division in this lineage. In this study we examine *tbx-2* and *egl-5*, genes that act in concert with *ham-1* to regulate HSN and PHB fate. In screens for mutants with abnormal HSN development, we identified the T-box protein TBX-2 as being important for both HSN and PHB differentiation. TBX-2, along with HAM-1, regulates the migrations of the HSNs and prevents the PHB neurons from adopting an apoptotic fate. The homeobox gene *egl-5* has been shown to regulate the migration and later differentiation of the HSN. While mutations that disrupt its function show no obvious role for EGL-5 in PHB development, loss of *egl-5* in a *ham-1* mutant background leads to PHB differentiation defects. Expression of EGL-5 in the HSN/PHB precursor but not in the PHB neuron suggests that EGL-5 specifies precursor fate. These observations reveal a role for both EGL-5 and TBX-2 in neural fate specification in the HSN/PHB lineage.

DEVELOPMENT relies on the intricate interplay between cell death, proliferation, migration, and differentiation to assure that proper numbers of cells are generated. The number of mitotic cells produced during development, for example, is balanced by both apoptosis and terminal differentiation. Asymmetric cell divisions have been shown to play an essential role in generating cells at the right time and place during animal development.

Several types of molecules have been implicated in the regulation of asymmetric cell divisions. Cell determinants such as Numb and Prospero are segregated to one daughter cell, causing it to adopt a particular fate (Uemura *et al.* 1989; Rhyu *et al.* 1994; Hirata *et al.* 1995; Knoblich *et al.* 1995; Rhyu and Knoblich 1995; Spana *et al.* 1995). Other molecules like Miranda regulate the distribution of the determinants (Ikeshima-Kataoka *et al.* 1997), and molecules like Inscutable control both the distribution of molecules like Miranda and orient the spindle so that determinants are inherited by a single daughter cell (Kraut and Campos-Ortega 1996; Kraut *et al.* 1996; Shen *et al.* 1997).

While much is known about the intrinsic molecules that control the asymmetric divisions of neuroblasts in Drosophila and of the *Caenorhabditis elegans* zygote, much less is known about how neuroblasts in *C. elegans* divide asymmetrically. Only two molecules, HAM-1 and PIG-1, are known to control both the sizes of daughter cells, presumably by controlling spindle position, and daughter cell fate of neuroblast divisions (Guenther and Garriga 1996; Frank *et al.* 2005; Cordes *et al.* 2006). One interesting feature of these molecules is that they function only in neuroblast lineages that produce apoptotic cells, such as the HSN/PHB lineage (Figure 1A). Mutations in these genes lead to the transformation of the cells fated to die into their sister cells, either neurons or neuronal precursors, leading to the production of extra neurons. A working model proposes that HAM-1 distributes developmental potential in the form of cell-fate determinants to the daughter cell that normally survives (Frank *et al.* 2005). If this model is correct, loss of these determinants should result in the loss of neurons in the affected divisions.

In this article, we describe two genes that are required for the production of the HSN and PHB neurons. In a screen for mutations that disrupt HSN development, we identified a mutant allele of *tbx-2*, which encodes a T-box protein of the TBX-2/3/4/5 family. T-box proteins have been shown to regulate cell-fate specification in multiple tissues (Naiche *et al.* 2005). We provide evidence suggesting that TBX-2 acts as a repressor of apoptosis for the PHB neuron. We also describe a new role for the Hox gene *egl-5* in the HSN/PHB lineage. Both *tbx-2* and *egl-5* regulate the specification of HSNs and PHBs,

[1]*Present address:* Department of Biochemistry and Biophysics, University of California, San Francisco, CA 94143-2822.

[2]*Corresponding author:* Department of Molecular and Cell Biology, 16 Barker Hall, University of California, Berkeley, CA 94720-3204. E-mail: garriga@berkeley.edu

and aspects of this regulation are revealed only in a *ham-1* mutant background. While our genetic observations are consistent with a role of TBX-2 and EGL-5 as determinants that regulate HSN and PHB development, we provide genetic evidence that suggests that these molecules may not be directly distributed by HAM-1.

## MATERIALS AND METHODS

**General procedure and strains:** Strains were grown at 20° and maintained as described (Brenner 1974). In addition to the wild-type strain N2, strains containing the following mutations and transgenes were used in this work:

LGI: *dpy-5(e61)* (Brenner 1974) *kyIs39 [Psra-6::gfp]* (Troemel *et al.* 1995); *ynIs45 [Pflp-15::gfp]* (Li *et al.* 1999; Kim and Li 2004); *zdIs5[mec-4::gfp]* (Clark and Chiu 2003).

LGII: *bli-2(e768)* (Brenner 1974); *gmIs20 [hlh-14::gfp]* (Frank *et al.* 2003); *gmIs13 [Psrb-6::gfp]* (this study).

LGIII: *dpy-17(e164)* (Brenner 1974); *tbx-2(ok529)* (Gene Knockout Consortium, http://celeganskoconsortium.omrf.org/); *tbx-2(gm111)* (this study); *egl-5(n945)* (Trent *et al.* 1983); *unc-32(e189)* (Brenner 1974); *gm345* (this study) *dpy-18(e364)* (Brenner 1974).

LGIV: *dpy-11(e224)* (Brenner 1974); *ham-1(n1438)* (Desai *et al.* 1988); *ham-1(gm279)* (Frank *et al.* 2005); *kyIs179 [Punc-86::gfp]* (Gitai *et al.* 2003).

LGV: *unc-5(e53)* (Brenner 1974); *gmIs22 [Pnlp-1::gfp]* (Li *et al.* 1999; Frank *et al.* 2003); *muIs13[egl-5::lacZ]* (Wang *et al.* 1993).

LGX: *lon-2(e678)* (Brenner 1974).

Rearrangements: *+/qC1[dpy-19(e1259) glp-1(q339)] III* (Graham and Kimble 1993); *+/mT1 II; +/mT1[dpy-10(e128)] III* (M. Edgley, personal communication).

Unmapped transgene: *AW0095 [tbx-2::gfp]* (A. Woollard, personal communication).

**Isolation and mapping of the *tbx-2(gm111)* and *gm345* mutations:** In a screen for mutations that disrupt HSN development, we mutagenized wild-type P0 hermaphrodites with 50 mM EMS for 4 hr and transferred individual $F_1$ hermaphrodite progeny to separate Petri plates. We then examined 15–20 $F_2$ progeny of individual $F_1$'s for HSN defects using Nomarski optics. One $F_1$ segregated arrested first larval stage (L1) progeny that lacked detectable HSNs by Nomarski optics. These animals also had either a "*P*harynx *un*attached" (Pun) phenotype or the pharynx was thin and abnormal in appearance.

We crossed wild-type males to hermaphrodites that segregated the L1 arrested phenotype. $F_1$ males were crossed to two strains, MT465 [*dpy-5; bli-2; unc-32*] and MT464 [*unc-5; dpy-11; lon-2*], and 10 $F_2$ L4 hermaphrodite cross progeny were isolated from each cross. For each cross, we chose an $F_2$ hermaphrodite that segregated L1 arrested animals and transferred 20 of its wild-type $F_3$ progeny to individual plates (the progeny were not Dpy, Bli, or Unc for the MT465 cross and were not Unc, Dpy, or Lon for the MT464 cross). For the MT464 cross, approximately two-thirds of the $F_3$ progeny segregated animals that displayed the L1 arrest, Unc, Dpy, or Lon phenotypes. For the MT465 cross, approximately two-thirds of the progeny segregated the Dpy and Bli phenotypes, but all 20 segregated the L1 arrest and Unc phenotype suggesting that the mutation causing the L1 arrest is linked to *unc-32*. The mutation responsible for this phenotype was named *gm111* and balanced by the *qC1* balancer chromosome.

We also generated *gm111/qC1* strains that contained a *gmIs13(srb-6::gfp)* transgene and noted that one of the phasmid neurons, which we later showed to be PHB, was missing ~91% of the time in *gm111* homozygous animals. This transgene was used in additional mapping experiments.

In a subsequent mapping experiment, we set out to order *gm111* relative to *dpy-17* and *unc-32* by building the strain *gmIs13/+; dpy-17 + unc-32/+ gm111 +* and isolating Unc, non-Dpy, and Dpy, non-Unc self progeny. All 15 of the Unc, non-Dpy progeny segregated L1 arrested animals. We were surprised to find that we could detect the HSNs in these arrested hermaphrodites, although the neurons were often misplaced. We also noted that while those strains that retained the *gmIs13* transgene were occasionally missing phasmid neurons, the penetrance of this defect was much higher in the original strain. We conclude that in these recombinant hermaphrodites we crossed off a linked modifier that enhanced the HSN and PHB defects caused by *gm111*.

Of the 20 Dpy non-Unc progeny, 3 were sterile. The remaining fertile hermaphrodites segregated dead embryos, arrested larvae and sterile as well as fertile adults. The arrested larvae and sterile adult progeny from each of the Dpy, non-Unc recombinant animals often had HSN migration defects and those that retained *gmIs13* in the background often had missing phasmid neurons. As with the arrested larvae from the Unc, non-Dpy recombinants, the penetrance of the phasmid neuron defect was higher in the original strain. Arrested L1 larvae were often Pun. From one of the Dpy, non-Unc recombinant progeny that contained *gmIs13*, we cloned 20 Dpy non-Unc fertile progeny, and they all segregated Dpy, Unc progeny, suggesting that when homozygous the recombinant chromosome resulted in the lethal and sterile phenotypes described above. Taken together, the mapping experiments suggest that the original strain contained two mutations: *gm111*, which mapped near or to the left of *dpy-17*, and a second mutation, which we named *gm345*, which maps near or to the right of *unc-32*. Alone, each mutation caused partially penetrant HSN and PHB phenotypes that were enhanced in the double mutant. The *gm111 unc-32* and *dpy-17 gm345* recombinant chromosomes were balanced over a *qC1* chromosome. Like the original double-mutant strain, *gm111* animals retained the Pun/abnormal pharynx phenotype.

To confirm our hypothesis that these two mutations caused the severe HSN defects, we crossed *gm111 gm345/qC1* males to *+ina-1 dpy-18/unc-32 +dpy-18* hermaphrodites and transferred individual non-Dpy progeny to separate plates. From $F_1$'s that segregated both the *unc-32 dpy-18* and the *gm111 gm345* chromosomes, we transferred 13 individual Dpy, non-Unc and six Unc Non-Dpy $F_2$ recombinant progeny to separate plates. All of the Dpy, non-Unc progeny segregated L1 arrested animals with misplaced HSNs, phenotypes associated with the *gm111* mutation. None of the Unc non-Dpy hermaphrodites segregated dead eggs, arrested larvae, or sterile adults. From these and the previous mapping experiments, we conclude that *gm345* maps near *unc-32*.

Our phenotypic analysis of *gm345* was conducted using a *dpy-17 gm345* recombinant chromosome that was isolated as described above. These mutant animals arrest at various stages of development, and those that make it to adulthood are sterile. Arrested L1 animals can display a Pun phenotype. Adult hermaphrodites can be vulvaless and less frequently multivulval. They also display HSN migration and PHB defects (data not shown). Presumably the *dpy-17* mutation does not contribute to the *gm345* mutant phenotypes. *gm345* is not considered further in this article.

Using the transgenic marker *gmIs13 (Psrb-6::gfp)* to detect the PHA and PHB neurons, we found that 91% of the sides scored in the *gm111 gm345* animals had a single neuron that

expressed GFP in arrested L1 hermaphrodites (Figure 2, A′–C′). Normally, each side of a *gmIs13* animal has two GFP-expressing cells in the tail, one PHB and one PHA, a second phasmid neuron that is unrelated linearly to the HSN. On the basis of the HSN phenotype and further analysis described below, we speculate that the arrested animals lacked PHBs.

*hlh-14* mutants lack HSNs, PHBs, and PVQ interneurons because the fate of the neuroblast that produces these cells is altered (Frank *et al.* 2003). To test whether the *gm111 gm345* L1 arrested animals also lacked PVQ neurons, we analyzed these mutant animals using the *kyIs39 (sra-6::gfp)* transgene marker (Troemel *et al.* 1995). Unlike *hlh-14* mutants, the arrested *gm111 gm345* L1 animals produced normal numbers of PVQs (data not shown). This observation suggests that the neuroblast that produces all three neurons is normal in these mutants.

**Complementation tests:** We noted that the *tbx-2(ok529)* mutation, which lies just to the right of *dpy-17*, caused an L1 arrest phenotype similar to that produced by the *gm111* mutation. Analysis of the HSN and phasmid neuron phenotypes of *tbx-2(ok529)* were also similar, increasing the likelihood that *gm111* is a *tbx-2* allele. To test this hypothesis, we crossed males heterozygous for the *kyIs179* HSN reporter into *tbx-2(ok529)/mT1* hermaphrodites. $F_1$ males carrying the reporter were crossed to *gm111 unc-32/qC1* hermaphrodites, and we scored cross progeny that contained the *kyIs179* transgene for the L1 arrest and HSN migration phenotypes of *tbx-2* mutants. Because this transgene often segregates away from the X chromosome, most of the progeny that contained the transgene were male and hence lacked HSNs. Of the 44 progeny scored, 29 had abnormal pharynxes similar to those seen in *ok529* and *gm111* animals. The frequency of animals with this defect was higher than one would expect and probably resulted from the bias introduced by picking L1 animals for the analysis by Nomarski and fluorescence microscopy. Because the mutant L1 animals arrest at this stage, with time these L1 mutants accumulate on the plate. Only 15 of the 44 animals were hermaphrodites: 11 of these had at least one HSN that was displaced. We concluded that *gm111* and *ok529* failed to complement and that *gm111* is a *tbx-2* allele.

**Strain constructions:** *ced-4 tbx-2; gmIs13: tbx-2* and *ced-4* are 0.31 MU apart on LGIII. *zdIs5/+*; *ced-4 dpy-17 unc-36/+++* males were crossed to *tbx-2(ok529)/qC1* hermaphrodites. Approximately 1000 $F_2$ cross progeny were picked from cross progeny plates that were of the genotype *zdIs5/+; ced-4 dpy-17+ unc-36/++ tbx-2(ok529)+*. Individual non-Unc, non-Dpy $F_3$ hermaphrodites with extra PLM neurons (26% of *ced-4* mutant animals have extra PLM neurons) were transferred to separate plates. The presence of *tbx-2(ok529)* in the next generation was verified by its Pun phenotype. We then constructed a strain containing *gmIs13* and the recombinant *ced-4 tbx-2* chromosome balanced by *qC1* using standard genetic techniques.

*tbx-2 egl-5; gmIs13: tbx-2* and *egl-5* are 1.51 MU apart on LGIII. Heterozygous *dpy-17 egl-5* males were crossed into *tbx-2(ok529)/ qC1* hermaphrodites, and ~60 individual $F_1$ progeny were transferred to separate plates. Hermaphrodites that segregated *dpy-17 egl-5* and *tbx-2(ok529)* were screened for non-Dpy Egl animals. The recombinant *tbx-2(ok529) egl-5(n945)* chromosome was balanced over *qC1* and subsequently crossed into *gmIs13*.

**Embryo fixation and staining:** Embryos were fixed and stained as described (Guenther and Garriga 1996). Primary antibodies used were rabbit polyclonal anti-GFP at 1:1000 dilution (Molecular Probes, Eugene, OR), mouse monoclonal anti-β-galactosidase at 1:500 dilution (Promega, Madison, WI) and mouse anti-EGL-43 at 1:2 dilution (Guenther and Garriga 1996). Secondary antibodies used were Alexa-488 goat antirabbit IgG, Alexa-568 goat antimouse, and Alexa-568 donkey antimouse (Molecular Probes), all at 1:100 dilution.

Imaging and scoring was done on a Zeiss Axioskop2 fluorescence compound microscope. Images were taken using an ORCA-ER CCD camera (Hammamatsu) and Openlab v.3.1 Imaging software (Improvision), and manipulated using Adobe Photoshop.

## RESULTS

***tbx-2* mutations:** The HSNs are a pair of bilaterally symmetric serotonergic motor neurons that innervate the vulval muscles and stimulate hermaphrodites to lay eggs (White *et al.* 1986; Desai *et al.* 1988). The HSNs are generated in the tail of the embryo by two HSN/PHB precursors that each divide to generate an HSN and a PHB phasmid chemosensory neuron (Figure 1, A and C). Shortly after being born, the HSNs of hermaphrodites migrate anteriorly to positions near the center of the embryo flanking the gonad primordium (Figure 1, B and C). In males, the HSNs die during this migration (Sulston *et al.* 1983). In hermaphrodites, the HSNs differentiate into serotonergic motor neurons during larval and adult stages (Desai *et al.* 1988). Using Nomarski optics, HSNs can be identified in their final positions in newly hatched L1 hermaphrodites. Mutants with defects in HSN development can often be identified as L1 animals with missing or misplaced HSNs (Desai *et al.* 1988).

To identify genes involved in HSN development, we used EMS mutagenesis and Nomarski microscopy in an $F_1$ clonal screen for HSN defects and identified an $F_1$ animal that segregated arrested L1 hermaphrodites that lacked any obvious HSNs. This phenotype can be caused by a failure to produce HSNs (Frank *et al.* 2003) or by the death of the HSNs (Desai *et al.* 1988), their fate in males. Alternatively, the HSNs can be produced, but then fail to migrate (Desai *et al.* 1988). When the HSNs fail to migrate from their birthplace in the tail, we cannot distinguish them from other neurons in the lumbar ganglion using Nomarski optics.

The L1 arrest and HSN phenotypes mapped to linkage group III. Three factor mapping of the mutant chromosome separated two linked mutations, *gm111* and *gm345*, that together contributed to the HSN and PHB phenotypes (Figures 2 and 3 and MATERIALS AND METHODS). The *gm111* mutation mapped near or to the left of *dpy-17* and caused the L1 arrest phenotype. In this article, we focus on the *gm111* mutation, and information on *gm345* is presented in MATERIALS AND METHODS. The arrested L1 *gm111* hermaphrodites had HSNs that could be detected by Nomarski optics, but they often arrested their migration prematurely and were displaced posteriorly (Figure 2, A–C, and Figure 3). Using the *kyIs179*(*Punc-86::gfp*) transgene as an HSN marker (Gitai *et al.* 2003), both the normally positioned and misplaced neurons expressed GFP, confirming that the

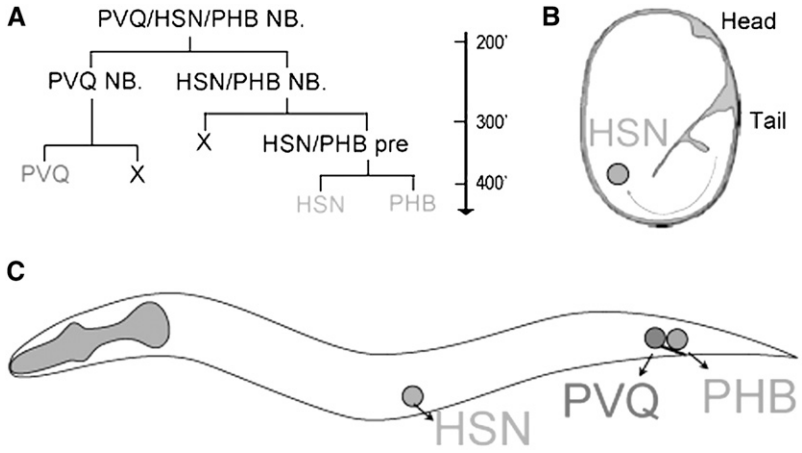


FIGURE 1.—HSN and PHB neuron development. (A) PVQ/HSN/PHB neuronal lineage. Vertical arrow represents time of development in minutes at 20°, beginning with the first embryonic cleavage at 0 min. NB stands for neuroblast and pre stands for precursor. (B) Schematic of an embryo showing the migration route of the HSN. Both the HSN and PHB are born in the tail of the developing embryo at about the stage shown in this diagram. (C) Schematic showing the positions of the HSN motor neuron, the chemosensory phasmid neuron PHB, and the interneuron PVQ in a newly hatched L1 hermaphrodite. Anterior is to the left, dorsal is up.

ectopic neurons identified by Nomarski optics were HSNs (Figure 2).

The gene *tbx-2* maps just to the right of *dpy-17*, and mutations in this gene cause an L1 arrest and pharyngeal phenotypes that were similar to those exhibited by *gm111* animals (ROY CHOWDHURI *et al.* 2006). Both *gm111* and the *tbx-2* mutation caused an L1 arrest phenotype that results from the inability of the animals to feed: the pharynx was often detached from the mouth (Pun phenotype), and those pharynxes that were attached were thin and abnormally shaped (Figure 4). We also found that *gm111* and *tbx-2(ok529)* mutants have similar HSN and PHB defects.

We assayed the PHB neurons in *gm111* and *tbx-2(ok529)* L1 arrested hermaphrodites using two different GFP markers: *gmIs13*, which expresses GFP in PHAs and PHBs (FRANK *et al.* 2003), and *gmIs22(nlp-1::GFP)*, which expresses GFP in the PHBs but not the PHAs (LI *et al.* 1999; FRANK *et al.* 2003). In both of these reporter backgrounds, *tbx-2(gm111)* and *tbx-2(ok529)* arrested animals had sides with missing cells (Figures 2C′ and 5A) suggesting that the mutation specifically affected PHB. Consistent with this interpretation, the PHA marker *ynIs45* (*flp-15::GFP*) revealed that the *tbx-2* mutants were not missing PHAs (LI *et al.* 1999; KIM and LI 2004) (data not shown).

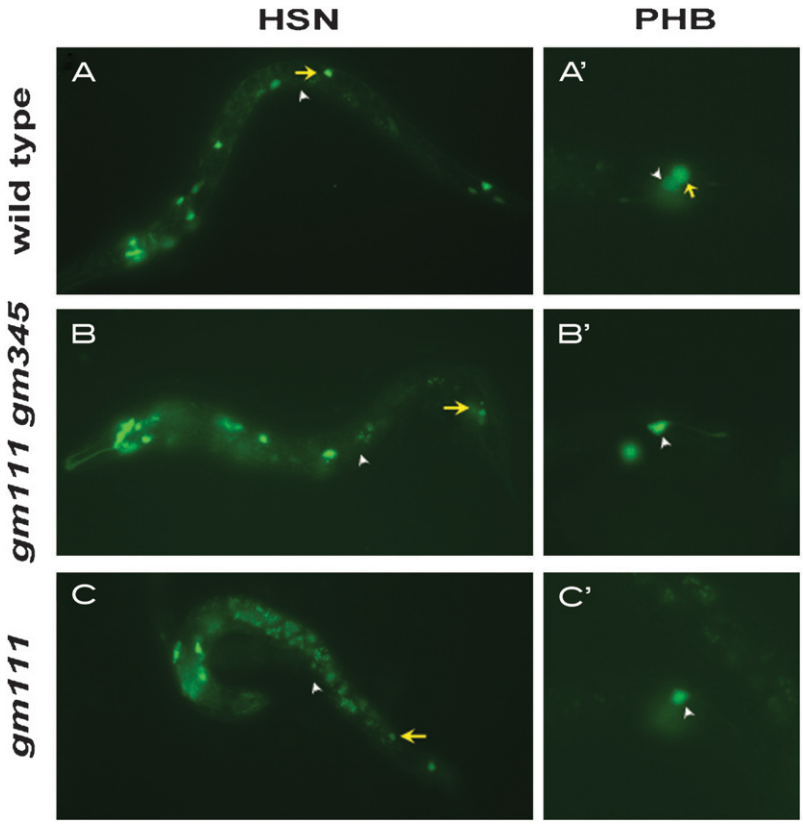


FIGURE 2.—HSN and PHB phenotypes in *tbx-2* and *tbx-2 gm345* hermaphrodites. The reporters *kyIs179* and *gmIs13* express GFP in the HSN (A–C) and the PHB (A′–C′), respectively. (A) *kyIs179*; (B) *gm111 gm345; kyIs179*; and (C) *gm111; kyIs179*. Anterior is to the left, dorsal is up. Arrows point to the HSN, and the arrowheads indicate the position of the center of the gonad primordium. In wild-type animals, the HSN lies lateral to the gonad and is displaced posteriorly along its migratory route in the two mutant backgrounds. (A′) *gmIs13*; (B′) *gmIs13; gm111 gm345*; and (C′) *gmIs13; tbx-2(gm111)*. Arrows point to the PHB, and the arrowheads point to the PHA. There is one PHA and one PHB on each side in wild-type animals and hence two GFP+ cells are seen on each side of the animal. Mutants are sometimes missing a PHB and in these cases have only one GFP+ cell, the PHA, on that side of the animal.

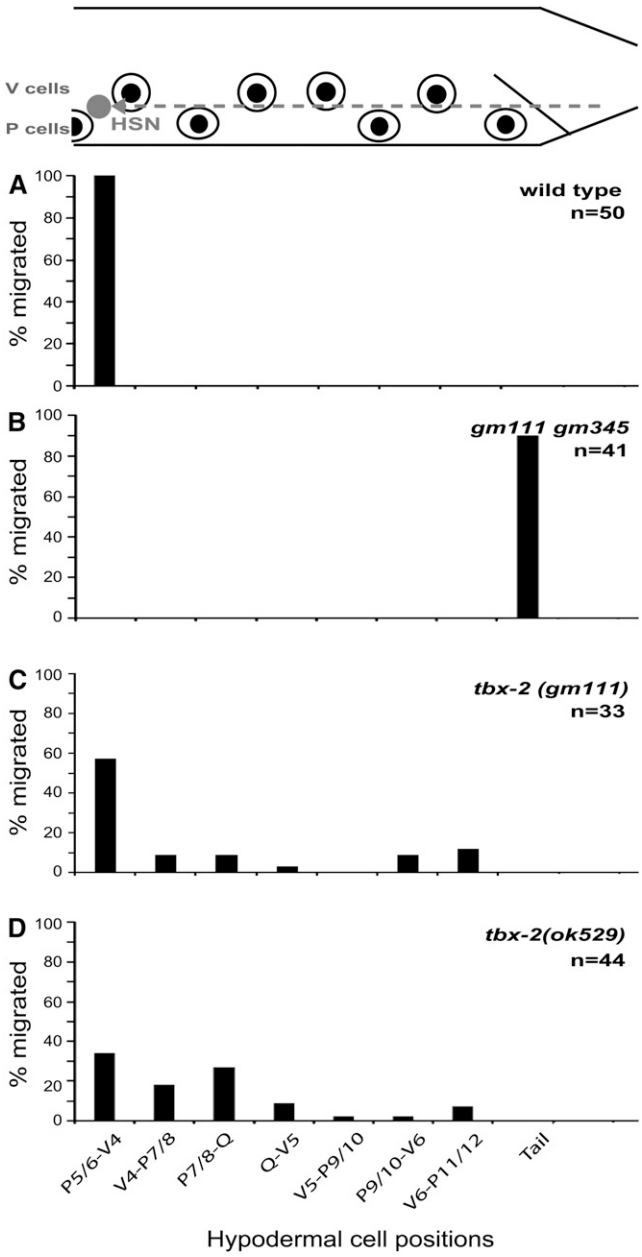


FIGURE 3.—*tbx-2* mutants have HSN migration defects. At the top is a schematic diagram of the posterior half of an L1 hermaphrodite. Anterior is to the left, dorsal is up. The dotted line represents the migratory route of the HSN. The positions of the V- and P-hypodermal cell nuclei are represented by eye-shaped structures, starting with P5/6 at the anteriormost position. The tick marks along each graph mark the position of the corresponding hypodermal cell aligned with respect to the diagram to the top. The *y*-axes of the graphs represent the percentage of neurons at each position along the anterior–posterior axis. *n* is the number of HSNs scored. All strains were scored with the reporter *kyIs179*. (A) Wild type, (B) *tbx-2(gm111) gm345*, (C) *tbx-2(gm111)*, and (D) *tbx-2(ok529)*.

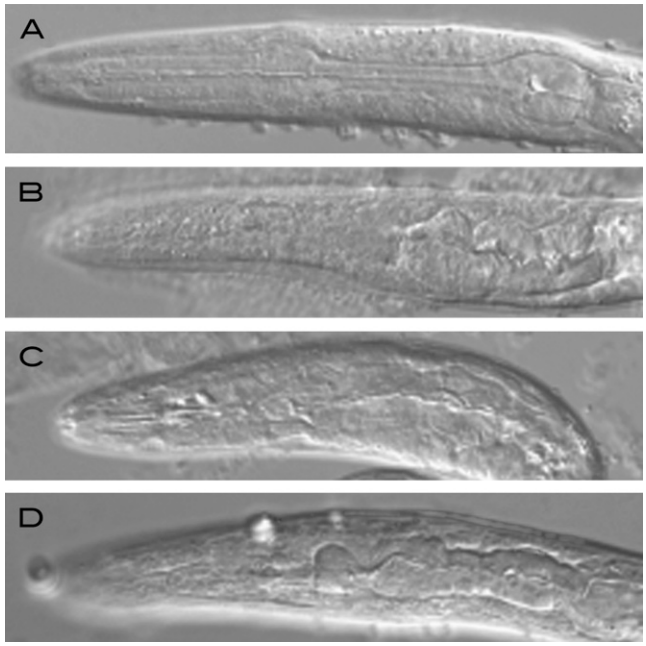


FIGURE 4.—Nomarski optic images of wild-type and mutant pharynxes. (A) Wild type, (B) *gm111 gm345*, (C) *tbx-2(gm111)*, and (D) *tbx-2(ok529)*. Anterior is to the left.

Complementation tests and sequencing confirmed that *gm111* is a *tbx-2* allele (MATERIALS AND METHODS). The *gm111* mutation is predicted to result in an Ala238Val change in the TBX-2 protein (Figure 6). Although this change is conservative, we speculate that it affects the ability of the protein to bind target DNA. The 10-amino-acid sequence flanking this Ala has been conserved across all T-box proteins (BOLLAG *et al.* 1994; PAPAIOANNOU and SILVER 1998), and analysis of vertebrate T-box protein/DNA cocrystals shows that this region and in particular Ala238 interacts with target DNA (MULLER and HERRMANN 1997; COLL *et al.* 2002). The deletion allele *tbx-2(ok529)* is a 1082-bp in-frame deletion that removes part of the conserved DNA binding domain, and genetic analysis suggests that the lesion eliminates *tbx-2* function (ROY CHOWDHURI *et al.* 2006; SMITH and MANGO 2007). The similarity of the *gm111* and *ok529* phenotypes indicates that *gm111* also results in a severe loss if not a total absence of TBX-2 function. Since *gm111* heterozygous animals show no mutant phenotype (data not shown), this mutation behaves like a severe recessive loss-of-function allele. All further analysis in this article was done with the predicted null allele *tbx-2(ok529)* unless otherwise specified.

**TBX-2 negatively regulates the cell-death pathway:** Two explanations can account for the missing PHB phenotype in *tbx-2* mutant animals. One is that TBX-2 negatively regulates cell death in the PHB neuron, such that in its absence, the PHB dies. The second is that TBX-2 regulates PHB differentiation, such that in its absence the PHB is born, but does not differentiate properly and thus does not express PHB markers. To distinguish between these possibilities, we blocked the execution of programmed cell death in a *tbx-2* mutant background and asked whether the missing PHB

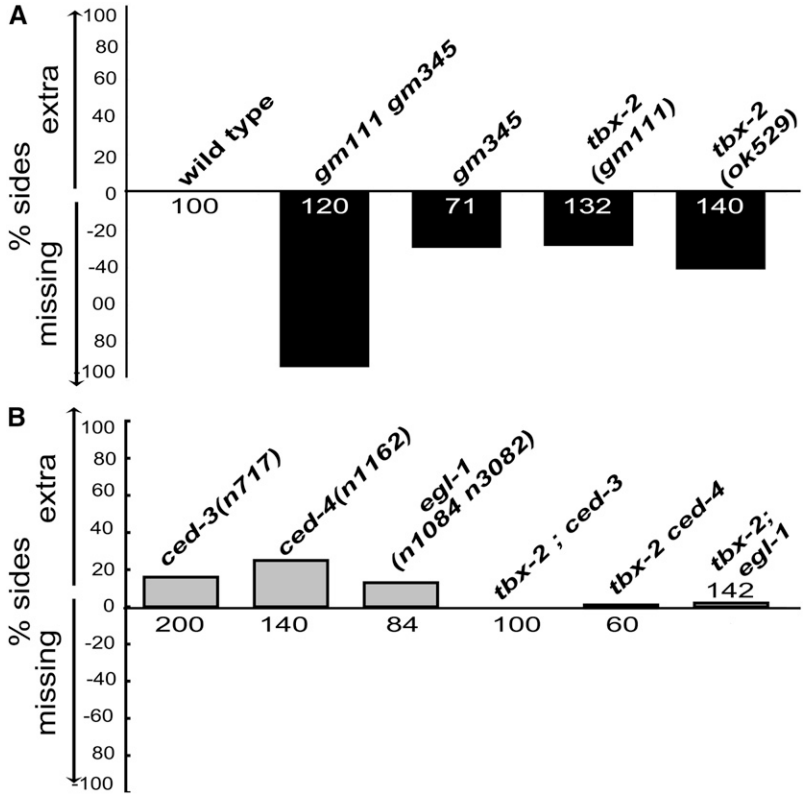


FIGURE 5.—PHB defects in *tbx-2(gm111) gm345*, *tbx-2(gm111)*, and *tbx-2(ok529)* mutants and their suppression by mutations in cell-death genes. The GFP reporter *gmIs13* was used to quantify the number of phasmid neurons. *Y*-axis denotes the percentage of sides scored with either an extra or a missing phasmid neuron. The number of sides scored are noted on the bars for each genotype. Genotypes are as indicated. (A) *tbx-2* mutants are missing phasmid neurons. (B) The missing cell phenotype of *tbx-2* mutants is rescued by mutations in genes that promote cell death. Double mutants using *ced-3*, *ced-4*, or *egl-1* were all built with *tbx-2(ok529)*.

phenotype could be rescued. If TBX-2 regulates cell death, then the prediction is that the missing PHB phenotype will be rescued. If, on the other hand, TBX-2 regulates PHB differentiation, then blocking the cell-death pathway should not affect the missing cell phenotype. *C. elegans* has a genetically defined core "apoptosis" execution pathway (METZSTEIN *et al.* 1998). Loss of the BH3-domain containing protein EGL-1, the Apaf-1 homolog CED-4, or the Caspase-9 homolog CED-3, completely rescued the "missing" cell phenotype of *tbx-2* mutants (Figure 5B). These observations suggest that TBX-2 functions as a negative regulator of the cell-death pathway for the *C. elegans* PHB neuron.

**TBX-2 AND HAM-1 independently regulate PHB development:** We previously had shown that the protein HAM-1 regulates the asymmetric division of the HSN/PHB lineage (GUENTHER and GARRIGA 1996; FRANK *et al.* 2005). Our hypothesis for its function, on the basis of its asymmetric cortical localization in the HSN/PHB neuroblast and on the *ham-1* mutant phenotypes, proposes that HAM-1 tethers cell-fate determinants in the HSN/PHB neuroblast, causing them to be inherited by the HSN/PHB precursor cell and excluding them from its anterior sister cell, which normally dies. In this model, loss of HAM-1 allows the equal distribution of the determinants into both daughters of the neuroblast, causing the anterior cell to divide and generate an extra HSN and PHB. *ham-1* mutants also have a low frequency of missing HSN and PHB neurons. We previously speculated that this loss of neurons could be due to a lower dose of determinants because they are now distributed between the two daughter cells.

This model predicts that loss of the determinants that specify HSN/PHB precursor fate would result in the loss of HSNs and PHBs. Alternatively, if several molecules are involved in specifying precursor fate, then the loss of one might result in the partial loss of these neurons, and the neuronal loss phenotype might be enhanced by loss of *ham-1*.

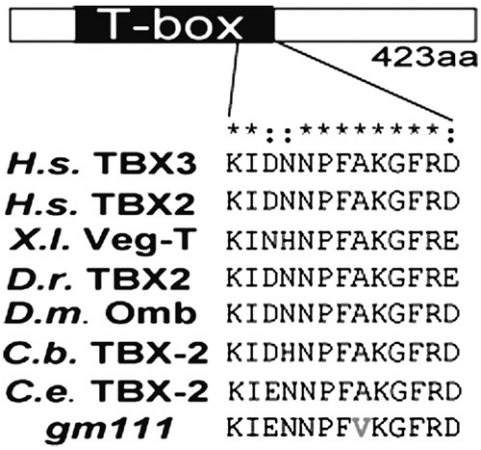


FIGURE 6.—*gm111* is a missense mutation that alters the conserved T-box binding domain. Alignment of a conserved 13-amino-acid sequence in Tbx2/3 orthologs from different species. *H.s.*, *Homo sapiens*; *X.l.*, *Xenopus laevis*; *D.r.*, *Danio rerio*; *D.m.*, *Drosophila melanogaster*; *C.b.*, *Caenorhabditis briggsae*; *C.e.*, *Caenorhabditis elegans*.

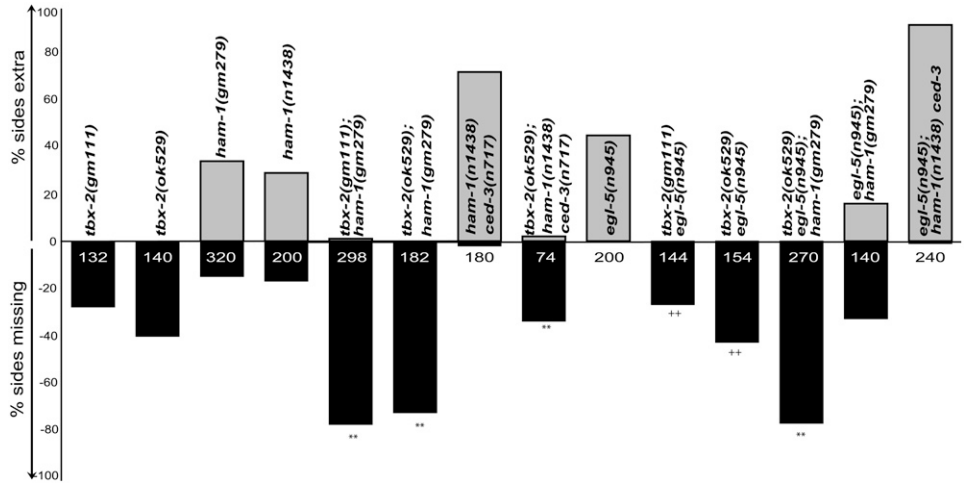


FIGURE 7.—HAM-1, EGL-5, and TBX-2 act in genetically parallel pathways to specify PHB fate. The GFP-reporter *gmIs13* was used to quantify the number of phasmid neurons. *Y*-axis denotes the percentage of sides scored with either an extra or a missing phasmid neuron. The number of sides scored is noted on the bars for each genotype. Genotypes are as indicated. Statistical significance is denoted as follows: (**) $P < 0.0001$ and (++) no significant difference between *tbx-2* and *tbx-2 egl-5* and no significant difference between *tbx-2 ham-1* and *tbx-2 egl-5; ham-1*.

We tested this model by constructing and analyzing *tbx-2; ham-1* double mutants. The strong loss-of-function alleles *ham-1(n1438)* and *ham-1(gm279)* result in some lineages that produce extra HSNs and PHBs and other lineages that fail to produce either neuron. Like the *tbx-2* HSN and PHB neuron-loss phenotype, the *ham-1* neuron-loss phenotype can be rescued by mutations in the cell-death pathway (GUENTHER and GARRIGA 1996; FRANK *et al.* 2005) (Figure 7 and data not shown). The missing neuron phenotype of the *tbx*-2 and *ham-1* mutants was significantly enhanced in *tbx-2(ok529); ham-1(gm279)* as well as *tbx-2(gm111); ham-1(gm279)* double mutants (Figure 7), suggesting that TBX-2 acts as a cell-fate determinant in the HSN/PHB lineage.

Because both TBX-2 and HAM-1 appear to regulate apoptosis in the HSN/PHB lineage, the simplest explanation for the large number of missing PHB neurons in *tbx-2; ham-1* double mutants is that either the PHBs or their precursors die. The explanation that the precursors or PHBs die, however, predicts that blocking apoptosis would suppress the missing PHB phenotype of *tbx-2; ham-1* mutants. Surprisingly, the *ced-3(n717)* mutation only partially suppressed this phenotype (Figure 7). This result suggests that besides playing a role in suppressing apoptosis, both TBX-2 and HAM-1 specify neural fate. We did not directly ask whether the missing cells scored in our assays die or whether they survive but do not express the GFP marker because of the difficulty in doing this experiment.

**The Hox protein EGL-5 also specifies neural fate in the HSN/PHB lineage:** Like the loss of TBX-2, loss of EGL-5 leads to HSN migration and differentiation defects (DESAI *et al.* 1988). The HSNs of *egl-5* mutants also express PHB markers such as *Psrb-6::gfp*, suggesting that the HSNs acquire differentiation traits of their sister cells (BAUM *et al.* 1999). *egl-5* mutants have no obvious PHB defect. These phenotypes and the observation that an *egl-5::lacZ* transgene is expressed in the HSN but not in the PHB suggest that EGL-5 is involved in specifying the fate of the HSN, and in its absence the HSN is partially transformed into its sister cell.

The observations described in the previous section suggest that a *ham-1* mutant can be used to sensitize the background for defects in PHB development. Even though *egl-5* mutants displayed no obvious PHB defect, we asked whether an *egl-5* mutation could perturb PHB development in a *ham-1* mutant background. We found that an *egl-5* mutation significantly enhanced the missing PHB phenotype of the *ham-1* mutant (Figure 7), revealing a role for EGL-5 in PHB development. It is noteworthy that the HSNs also failed to express the *Psrb-6::gfp* transgene in the double mutants. This latter observation and the lack of *egl-5* expression in PHB raised the possibility that EGL-5 does not control PHB development directly, but rather regulates the fate of the HSN/PHB precursor. We tested this hypothesis by asking whether the HSN/PHB precursor expressed the *egl-5::lacZ* transgene, *muIs13* (WANG *et al.* 1993). The GFP reporter *gmIs20 (hlh-14::GFP)* is expressed in the HSN/PHB neuroblast as well as its daughter cell, the HSN/PHB precursor, providing a marker for cells in the lineage (FRANK *et al.* 2003). We generated a *muIs13 (egl-5::lacZ); gmIs20 (hlh14::GFP)* strain, and costained the embryos with anti-β-galactosidase and anti-GFP antibodies. We saw that the neuroblast stained positive only for GFP (data not shown). By contrast, we did see costaining of the precursor cell with both anti-β-galactosidase and anti-GFP antibodies (Figure 8, A–D). This costaining was lost around the time when the precursor divides and also was missing in the HSN neuron, which stained only for β-galactosidase (data not shown). These observations show that *egl-5* is expressed in the HSN/PHB precursor, and then later only in the HSN. Thus, EGL-5 is likely to function in two cells of the lineage. We propose that EGL-5 functions early in the HSN/PHB precursor to regulate its fate and then later in the HSN to specify its fate, making it different from its PHB sister cell. Some of the HSN defects of *egl-5* mutants could be a consequence of HSN/PHB precursor abnormalities.

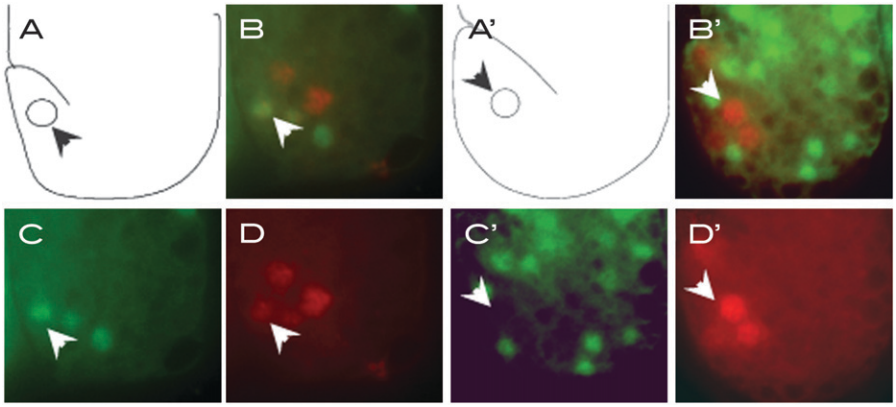


Figure 8.—EGL-5 is expressed in the HSN/PHB precursor, while TBX-2 is not. (A–D) *gmIs20[hlh-14::gfp]; muIs13[egl-5::lacZ]* representative embryo around the 1.5-fold stage stained with anti-GFP (green) and anti-lacZ (red). (A) Schematic of embryo; (B) merge of anti-gfp and anti-lacZ; (C) anti-GFP; and (D) anti-lacZ. (A′–D′) *muIs13[egl-5::lacZ]; AW0095[tbx-2::gfp]* representative embryo around the 1.5-fold stage stained with anti-GFP (green) and anti-lacZ (red). (A′) Schematic of embryo; (B′) merge of anti-gfp and anti-lacZ; (C′) anti-GFP; and (D′) anti-lacZ of a representative embryo.

The missing cell phenotype of the *ham-1; egl-5* double mutant could be due to either improper cell-fate specification or inappropriate cell death. Furthermore, both HAM-1 and EGL-5 could regulate fate or death in the precursor, in the HSN, or PHB neurons, or in both the precursor and the neurons. Approximately 27 and 15% of the HSN neurons are missing in *egl-5* and *ham-1* hermaphrodites, respectively. Both of these missing cell defects can be rescued by mutations in *ced-3* (Guenther and Garriga 1996; Baum *et al.* 1999).

To further analyze the *ham-1; egl-5* missing cell defect, we built a *egl-5(n945); ham-1(n1438) ced-3(n717)* triple mutant. We predicted that if the missing cell defect was entirely due to improper cell-fate specification of the PHB or the precursor (*i.e.*, inability to express the *Psrb-6::gfp* marker), the triple mutant would resemble *ham-1; egl-5* double mutants and be refractory to rescue with *ced-3*. Alternately, if cell death of the precursor and/or the HSN/PHB neurons caused the missing cell defects, we should see a rescue of the phenotype. The triple mutant *egl-5(n945); ham-1(n1438) ced-3(n717)* had a penetrant extra PHB phenotype (Figure 7). This is not merely a rescue of the missing PHB defect of the *ham-1; egl-5* double, but rather a synergistic enhancement of the number of cells expressing *Psrb-6::gfp*. In many cases we saw two extra PHB neurons, and in some cases, even three extra neurons per side (data not shown). This presence of four "PHB-like" neurons could result if both the apoptotic cell is transformed into its sister, the HSN/PHB precursor, and the HSNs adopt traits of their sister PHB neurons. The phenotype of the triple mutant suggests that both HAM-1 and EGL-5 regulate the survival and fate of the precursor, and the HSN and PHB neurons.

***tbx-2* mutations are epistatic to *egl-5*:** If TBX-2 regulates PHB fate, we predict that its function would be required for the HSN of *egl-5* mutants to express PHB-like traits. This is indeed the case. The ectopic expression of *srb-6::gfp* in *egl-5* HSNs is lost in *tbx-2 egl-5(n945)* double mutants (Figure 7). These data corroborate the hypothesis that TBX-2 specifies "PHB fate."

The results described above suggest that HAM-1 and EGL-5 work in parallel to regulate the fate of the precursor cell. On the basis of the lack of any obvious *egl-5::lacZ* expression in the PHB, we propose that EGL-5 acts in the precursor to specify its fate, and when the precursor divides, EGL-5 function becomes restricted to its anterior daughter, the HSN. In the HSN, EGL-5 represses PHB fate, while TBX-2 specifies PHB differentiation in the posterior daughter cell. If this model is correct, then the PHB fate defects of *tbx-2; ham-1* mutants should not be enhanced by the presence of an *egl-5* mutation. Indeed, the PHB defects of *tbx-2 egl-5; ham-1* triple mutants did not look any worse than those of *tbx-2; ham-1* double mutants (Figure 7). We also predicted that *ham-1* should enhance the *tbx-2 egl-5* PHB defects, since it functions higher in the lineage to specify the precursor fate. Indeed, comparing the triple mutant with *tbx-2 egl-5* shows a strong enhancement of the PHB phenotype (Figure 7).

**A *tbx-2::gfp* transgene is not expressed in the HSN/PHB precursor:** We propose that TBX-2 is a regulator of PHB fate. Does it function in the PHB neuron to specify its fate? To test whether a *tbx-2::gfp* transgene is expressed within the HSN/PHB lineage, we carried out similar colabeling experiments as described above. Having established that the *egl-5::lacZ* transgene is expressed in the precursor cell, we costained a strain carrying *tbx-2::gfp* (Roy Chowdhuri *et al.* 2006) and *muIs13* with both anti-GFP and anti-β-galactosidase antibodies. We saw no colabeling of the HSN/PHB precursor, suggesting that TBX-2 may not be expressed at that time (Figure 8, A′–D′). We also ruled out coexpression of *tbx-2::gfp* with antibodies to EGL-43, which stain the HSN and PHB, or with antibodies to HAM-2, which stain the HSN (data not shown). Thus, we have been unable to detect expression of *tbx-2::gfp* in any cells of the HSN/PHB lineage.

This observation leaves us with three possibilities. First, TBX-2 is normally expressed in the HSN/PHB lineage, but the TBX-2::GFP levels were too low to detect or were expressed transiently and were not detected in our experiments, Second, the TBX-2::GFP may not be expressed appropriately from this transgene, at least in cells required for the L1 arrest and HSN phenotypes. However, this transgene did rescue the PHB defects,

suggesting that it should be expressed in cells involved in regulation of PHB fate (data not shown) (Roy Chowdhuri *et al.* 2006; Smith and Mango 2007). Third, TBX-2 could function cell nonautonomously outside the lineage to regulate HSN and PHB differentiation.

**TBX-2 acts in parallel to HAM-1 and EGL-5 to regulate HSN migration:** *ham-1* is a gene that is required for HSN migration (Desai *et al.* 1988). Since our data suggest that TBX-2 and HAM-1 work in parallel to regulate PHB cell fate, we wondered if the two genes work in a similar manner to regulate HSN migration. The double mutant *tbx-2(ok529); ham-1(gm279)* shows strongly synergistic HSN migration defects, suggesting that as with PHB development, the two genes operate in parallel genetic pathways for HSN migration as well (Figure 9).

While mutations in *tbx-2* are epistatic to a mutation in *egl-5* for the PHB differentiation defects (Figure 7), we found that they are synergistic for the HSN migration defects (Figure 9). We conclude that TBX-2 and EGL-5 function independently to regulate HSN migration.

**HSN defects in *tbx-2* are independent of the PHB differentiation defects:** Mutations in *tbx-2* regulate the fate of both the PHB and the HSN. To address whether the HSN migration defects could result from the absence of the PHB neuron, we scored the HSN positions in *tbx-2(ok529); ced-3(n717)* double mutants. The HSN migration defects are not rescued in these mutants (Figure 9), suggesting that the HSN migration defects are not a secondary consequence of the loss of the PHB neuron.

## DISCUSSION

In a screen for HSN migration mutants, we identified the gene encoding the T-box transcription factor TBX-2 as a regulator of HSN and PHB differentiation. *C. elegans* TBX-2 is the only *C. elegans* ortholog of the TBX-2/3/4/5 subfamily of T-box proteins (Agulnik *et al.* 1995). This class of proteins has been implicated in the specification of various tissues during embryonic development across various species, including humans (Davenport *et al.* 2003; Harrelson *et al.* 2004; Jerome-Majewska *et al.* 2005; Manning *et al.* 2006).

While this class of T-box proteins appears to act in multiple pathways, they often act downstream of BMP signaling and upstream of FGF signaling (Naiche *et al.* 2005; Manning *et al.* 2006). Since the TGFβ-receptors DAF-1 and DAF-4 are expressed in the phasmid neuron PHB (Gunther *et al.* 2000), it will be interesting to test whether *daf-4* regulates PHB development and is genetically epistatic to *tbx-2*.

TBX-2 has been shown to coordinate migration of neural and neuroectodermal cells in zebrafish by mediating the downregulation of cadherins by Wnts (Fong *et al.* 2005). All five of the *C. elegans* Wnts contribute to HSN migration (Pan *et al.* 2006), raising the interesting possibility that *tbx-2* could either be a target of Wnt signaling or regulate a Wnt signaling compo-

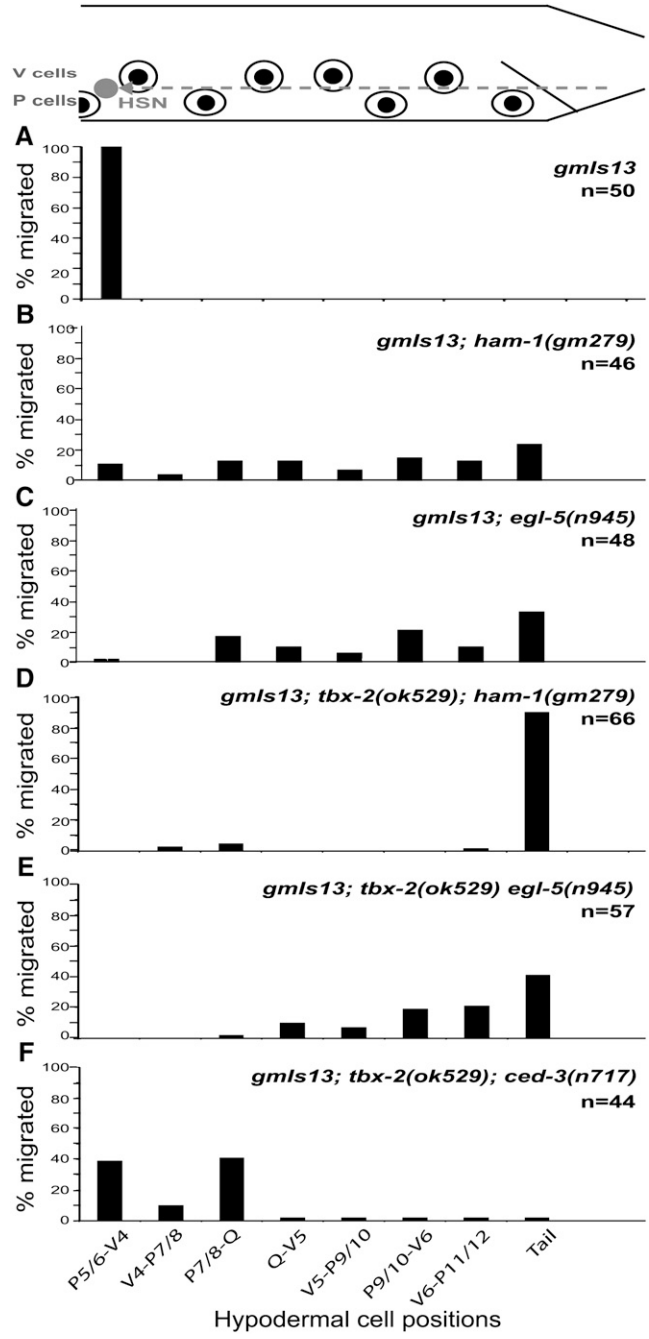


Figure 9.—HSN migration defects in double mutants. At the top is a schematic of the posterior half of an L1 hermaphrodite. Anterior is to the left, dorsal is up. The dotted line represents the migratory route of the HSN. The positions of the V- and P-hypodermal cell nuclei are represented by eye-shaped structures, starting with P5/6 at the anteriormost position. The tick marks along each graph mark the position of the corresponding hypodermal cell aligned with respect to the diagram to the top. The *y*-axes of the graphs represent the percentage of neurons at each position along the anterior–posterior axis. *ced-3* mutants have no HSN migration defects (not shown). (A) *gmIs13*; (B) *gmIs13; ham-1(n1438)*; (C) *gmIs13; egl-5(n945)*; (D) *gmIs13; tbx-2(ok529); ham-1(gm279)*; (E) *gmIs13; tbx-2(ok529) egl-5(n945)*; and (F) *gmIs13; tbx-2(ok529); ced-3(n717). n*, the number of HSNs scored, is indicated along graphs for each genotype.

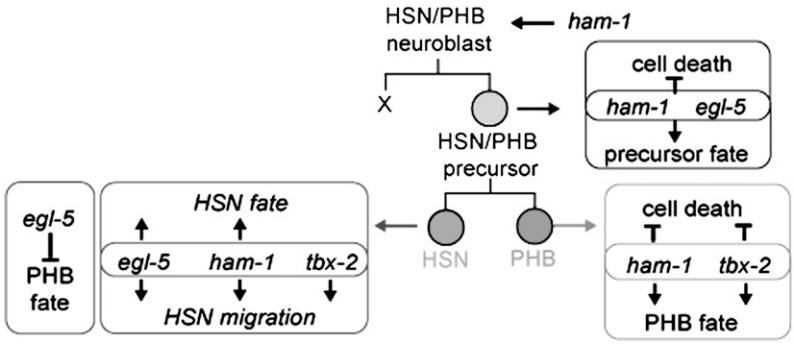


Figure 10.—Model summarizing genetic data implicating TBX-2, HAM-1, and EGL-5 as regulators of the survival and fate of the precursor cell, the HSN neuron, and the PHB neuron, as well as migration of the HSN neuron. We propose that *egl-5* acts to promote HSN development and to inhibit PHB fate in the HSNs. These models are not mutually exclusive. By inhibiting PHB fate, for example, *egl-5* could promote the expression of HSN traits.

nent. For example, this may predict that migration defects in *tbx-2* will not be enhanced by mutations in Wnt components. Consistent with this idea, *tbx-2(ok529)* does not enhance HSN migration defects of the *C. elegans* Wnt, *egl-20* (data not shown).

In *C. elegans,* TBX-2 is implicated in the regulation of ABa-derived anterior pharyngeal muscles (Roy Chowdhuri *et al.* 2006; Smith and Mango 2007). TBX-2 has been shown to interact with the SUMO-conjugating enzyme UBC-9 and to interact genetically in a positive feedback loop with the FoxA transcription factor PHA-4 for commitment to pharyngeal muscle fate.

*In vitro* cell culture and mouse model studies link TBX-2/3 to the cell cycle and cellular senescence via the p19/ARF pathway (Jacobs *et al.* 2000; Brummelkamp *et al.* 2002; Lingbeek *et al.* 2002; Prince *et al.* 2004; Jerome-Majewska *et al.* 2005). It is yet unclear whether TBX-2 controls these phenotypes by regulating genes involved in apoptosis, cell proliferation, or both. Our analysis suggests that in *C. elegans,* TBX-2 regulates apoptosis in the PHB neuron.

The genetic interactions between TBX-2 and cell-death genes indicate that TBX-2 functions as a negative regulator of apoptosis for the *C. elegans* PHB neuron. This role of TBX-2 may be similar to the role of vertebrate Tbx3 in regulating apoptosis/senescence of rat bladder epithelial-cell carcinomas (Brummelkamp *et al.* 2002; Ito *et al.* 2005) and distinct from its role in pharyngeal muscle development in *C. elegans.* Thus the role of TBX-2 in the PHB neuron may provide a model genetic system to probe the mechanism of its interaction with the apoptotic machinery. In this context, it is noteworthy that the gene *egl-1,* which encodes a BH3-like protein that activates the *C. elegans* cell-death pathway, has a cluster of seven putative T-box binding sites within the sequence upstream of the transcription start site for *egl-1* (A. Garnett, personal communication). It is also possible that the role of TBX-2 in regulating HSN migration is analogous to the role of vertebrate Tbx2/3 in regulating cell migrations (Naiche *et al.* 2005).

Mutations in *tbx-2* affect both the HSN and PHB sister neurons. For several reasons, we suspect that rather than acting at the level of the HSN/PHB precursor, TBX-2 acts independently to regulate HSN and PHB fates (Figure 10). First, while TBX-2 regulates PHB survival, it does not appear to regulate the survival of the precursor cell or of the HSN. Second, mutations in the apoptotic machinery can rescue the missing PHB defect, but do not rescue the HSN migration defect (Figure 9). This difference also indicates that the HSN migration defect is not a secondary consequence of missing PHBs. Third, the penetrance of the two phenotypes is different, and we have seen no obvious correlation between the HSN and PHB phenotypes. Sides missing PHBs, for example, can have normally positioned or misplaced HSNs (data not shown).

Genetic interactions suggest that TBX-2 and HAM-1 function in parallel to regulate the HSN/PHB lineage (Figure 10). HAM-1 has previously been shown to localize asymmetrically to the cell cortex of the HSN/PHB neuroblast and to be inherited by the HSN/PHB precursor. Because the daughter cell that does not inherit HAM-1 is transformed in *ham-1* mutants, we proposed that HAM-1 acts as a tether that segregates cell-fate determinants asymmetrically to the precursor (Guenther and Garriga 1996; Frank *et al.* 2005). But *ham-1* mutants occasionally are missing HSNs and PHBs. To explain this phenotype in the context of the tether model, we propose that when determinants are distributed to both cells in the mutant, their levels can fall below a threshold necessary for neural specification. This model predicts that loss of genes involved in HSN and PHB specification will synergize with *ham-1* mutations to generate a highly penetrant missing cell phenotype. Consistent with this prediction, *tbx-2; ham-1* double mutants are strongly synergistic and lack PHB neurons ~75–80% of the time. The mutations in the two genes are also strongly synergistic for HSN migration: we never detect the HSNs in their normal positions and rarely detect them along their migration route in *tbx-2; ham-1* double mutants.

We also found that the loss of PHB neurons caused by *ham-1* mutations was enhanced by loss of *egl-5.* EGL-5 is a Hox protein that specifies the fates of several cells located in the tail of the worm (Chisholm 1991; Clark *et al.* 1993; Wang *et al.* 1993). EGL-5 is crucial for HSN development, controlling its ability to migrate during embryonic development and its later differentiation

during larval and adult stages of development (Desai *et al.* 1988). EGL-5 acts by activating the *ham-2* and *unc-86* transcription factor genes. In the absence of *egl-5* or both *ham-2* and *unc-86*, the HSN takes on traits of its sister cell, the PHB (Baum *et al.* 1999). Consistent with the model that TBX-2 regulates PHB fate, *tbx-2* is required for *egl-5* HSNs to express PHB markers. By contrast, *tbx-2* mutations enhanced the HSN defects of *egl-5* mutants. These data together lead us to propose that TBX-2 has two independent functions in the HSN/PHB lineage: to repress cell death and activate cell differentiation in the PHB and to promote HSN migration in parallel to EGL-5 (Figure 10).

Any further understanding of the genetic interactions among the *ham-1, egl-5*, and *tbx-2* genes will require an analysis of whether HAM-1 regulates the expression or distribution of TBX-2 or EGL-5. The tools for this type of study are currently lacking.

The role of EGL-5 in PHB development that was revealed in the *egl-5; ham-1* double mutant supports the idea that *ham-1* mutants may provide a unique background to discover genes involved in HSN and PHB development. Both the HSN and PHB defects are also much more severe in *gm345; ham-1* double mutants than in either of the single mutants (data not shown). All of these observations taken together suggest that *ham-1* mutants can function as a sensitizing background to identify genes involved in HSN and PHB specification. *ham-1* mutations are pleiotropic, affecting many asymmetric neuroblast divisions that generate neurons and apoptotic cells in the embryo (Guenther and Garriga 1996; Frank *et al.* 2005). We therefore believe that the *ham-1* mutant might provide a useful background to identify neural specification genes for neurons arising from all these lineages.

We thank Alison Woollard and Pete Okkema for strains. We thank Aaron Garnett for *in silico* analysis of the *egl-1* promoter sequence for consensus T-box binding sites. We also thank Shaun Cordes for many helpful discussions and suggestions and Aaron Garnett for comments on the manuscript. Some nematode strains used in this work were provided by the Caenorhabditis Genetics Center, which is funded by the National Institutes of Health (NIH) National Center for Research Resources. This work was supported by NIH grant NS-42213 to G.G.

## LITERATURE CITED

Agulnik, S. I., R. J. Bollag and L. M. Silver, 1995 Conservation of the T-box gene family from Mus musculus to Caenorhabditis elegans. Genomics **25:** 214–219.

Baum, P. D., C. Guenther, C. A. Frank, B. V. Pham and G. Garriga, 1999 The Caenorhabditis elegans gene ham-2 links Hox patterning to migration of the HSN motor neuron. Genes Dev. **13:** 472–483.

Bollag, R. J., Z. Siegfried, J. A. Cebra-Thomas, N. Garvey, E. M. Davison *et al.*, 1994 An ancient family of embryonically expressed mouse genes sharing a conserved protein motif with the T locus. Nat. Genet. **7:** 383–389.

Brenner, S., 1974 The genetics of Caenorhabditis elegans. Genetics **77:** 71–94.

Brummelkamp, T. R., R. M. Kortlever, M. Lingbeek, F. Trettel, M. E. MacDonald *et al.*, 2002 TBX-3, the gene mutated in ulnar-mammary syndrome, is a negative regulator of p19ARF and inhibits senescence. J. Biol. Chem. **277:** 6567–6572.

Chisholm, A., 1991 Control of cell fate in the tail region of C. elegans by the gene egl-5. Development **111:** 921–932.

Clark, S. G., A. D. Chisholm and H. R. Horvitz, 1993 Control of cell fates in the central body region of C. elegans by the homeobox gene lin-39. Cell **74:** 43–55.

Clark, S. G., and C. Chiu, 2003 C. elegans ZAG-1, a Zn-finger-homeodomain protein, regulates axonal development and neuronal differentiation. Development **130:** 3781–3794.

Coll, M., J. G. Seidman and C. W. Muller, 2002 Structure of the DNA-bound T-box domain of human TBX3, a transcription factor responsible for ulnar-mammary syndrome. Structure **10:** 343–356.

Cordes, S., C. A. Frank and G. Garriga, 2006 The C. elegans MELK ortholog PIG-1 regulates cell size asymmetry and daughter cell fate in asymmetric neuroblast divisions. Development **133:** 2747–2756.

Davenport, T. G., L. A. Jerome-Majewska and V. E. Papaioannou, 2003 Mammary gland, limb and yolk sac defects in mice lacking Tbx3, the gene mutated in human ulnar mammary syndrome. Development **130:** 2263–2273.

Desai, C., G. Garriga, S. L. McIntire and H. R. Horvitz, 1988 A genetic pathway for the development of the Caenorhabditis elegans HSN motor neurons. Nature **336:** 638–646.

Fong, S. H., A. Emelyanov, C. Teh and V. Korzh, 2005 Wnt signalling mediated by Tbx2b regulates cell migration during formation of the neural plate. Development **132:** 3587–3596.

Frank, C. A., P. D. Baum and G. Garriga, 2003 HLH-14 is a C. elegans Achaete-Scute protein that promotes neurogenesis through asymmetric cell division. Development **130:** 6507–6518.

Frank, C. A., N. C. Hawkins, C. Guenther, H. R. Horvitz and G. Garriga, 2005 C. elegans HAM-1 positions the cleavage plane and regulates apoptosis in asymmetric neuroblast divisions. Dev. Biol. **284:** 301–310.

Gitai, Z., T. W. Yu, E. A. Lundquist, M. Tessier-Lavigne and C. I. Bargmann, 2003 The netrin receptor UNC-40/DCC stimulates axon attraction and outgrowth through enabled and, in parallel, Rac and UNC-115/AbLIM. Neuron **37:** 53–65.

Graham, P. L., and J. Kimble, 1993 The mog-1 gene is required for the switch from spermatogenesis to oogenesis in Caenorhabditis elegans. Genetics **133:** 919–931.

Guenther, C., and G. Garriga, 1996 Asymmetric distribution of the C. elegans HAM-1 protein in neuroblasts enables daughter cells to adopt distinct fates. Development **122:** 3509–3518.

Gunther, C. V., L. L. Georgi and D. L. Riddle, 2000 A Caenorhabditis elegans type I TGF beta receptor can function in the absence of type II kinase to promote larval development. Development **127:** 3337–3347.

Harrelson, Z., R. G. Kelly, S. N. Goldin, J. J. Gibson-Brown, R. J. Bollag *et al.*, 2004 Tbx2 is essential for patterning the atrioventricular canal and for morphogenesis of the outflow tract during heart development. Development **131:** 5041–5052.

Hirata, J., H. Nakagoshi, Y. Nabeshima and F. Matsuzaki, 1995 Asymmetric segregation of the homeodomain protein Prospero during Drosophila development. Nature **377:** 627–630.

Ikeshima-Kataoka, H., J. B. Skeath, Y. Nabeshima, C. Q. Doe and F. Matsuzaki, 1997 Miranda directs Prospero to a daughter cell during Drosophila asymmetric divisions. Nature **390:** 625–629.

Ito, A., M. Asamoto, N. Hokaiwado, S. Takahashi and T. Shirai, 2005 Tbx3 expression is related to apoptosis and cell proliferation in rat bladder both hyperplastic epithelial cells and carcinoma cells. Cancer Lett. **219:** 105–112.

Jacobs, J. J., P. Keblusek, E. Robanus-Maandag, P. Kristel, M. Lingbeek *et al.*, 2000 Senescence bypass screen identifies TBX2, which represses Cdkn2a (p19(ARF)) and is amplified in a subset of human breast cancers. Nat. Genet. **26:** 291–299.

Jerome-Majewska, L. A., G. P. Jenkins, E. Ernstoff, F. Zindy, C. J. Sherr *et al.*, 2005 Tbx3, the ulnar-mammary syndrome gene, and Tbx2 interact in mammary gland development through a p19Arf/p53-independent pathway. Dev. Dyn. **234:** 922–933.

Kim, K., and C. Li, 2004 Expression and regulation of an FMRFamide-related neuropeptide gene family in Caenorhabditis elegans. J. Comp. Neurol. **475:** 540–550.

Knoblich, J. A., L. Y. Jan and Y. N. Jan, 1995 Asymmetric segregation of Numb and Prospero during cell division. Nature **377:** 624–627.

Kraut, R., and J. A. Campos-Ortega, 1996 inscuteable, a neural precursor gene of Drosophila, encodes a candidate for a cytoskeleton adaptor protein. Dev. Biol. **174:** 65–81.

Kraut, R., W. Chia, L. Y. Jan, Y. N. Jan and J. A. Knoblich, 1996 Role of inscuteable in orienting asymmetric cell divisions in Drosophila. Nature **383:** 50–55.

Li, C., K. Kim and L. S. Nelson, 1999 FMRFamide-related neuropeptide gene family in Caenorhabditis elegans. Brain Res. **848:** 26–34.

Li, C., L. S. Nelson, K. Kim, A. Nathoo and A. C. Hart, 1999 Neuropeptide gene families in the nematode Caenorhabditis elegans. Ann. NY Acad. Sci. **897:** 239–252.

Lingbeek, M. E., J. J. Jacobs and M. van Lohuizen, 2002 The T-box repressors TBX2 and TBX3 specifically regulate the tumor suppressor gene p14ARF via a variant T-site in the initiator. J. Biol. Chem. **277:** 26120–26127.

Manning, L., K. Ohyama, B. Saeger, O. Hatano, S. A. Wilson *et al.*, 2006 Regional morphogenesis in the hypothalamus: a BMP-Tbx2 pathway coordinates fate and proliferation through Shh downregulation. Dev. Cell **11:** 873–885.

Metzstein, M. M., G. M. Stanfield and H. R. Horvitz, 1998 Genetics of programmed cell death in C. elegans: past, present and future. Trends Genet. **14:** 410–416.

Muller, C. W., and B. G. Herrmann, 1997 Crystallographic structure of the T domain-DNA complex of the Brachyury transcription factor. Nature **389:** 884–888.

Naiche, L. A., Z. Harrelson, R. G. Kelly and V. E. Papaioannou, 2005 T-box genes in vertebrate development. Annu. Rev. Genet. **39:** 219–239.

Pan, C. L., J. E. Howell, S. G. Clark, M. Hilliard, S. Cordes *et al.*, 2006 Multiple Wnts and frizzled receptors regulate anteriorly directed cell and growth cone migrations in Caenorhabditis elegans. Dev. Cell **10:** 367–377.

Papaioannou, V. E., and L. M. Silver, 1998 The T-box gene family. BioEssays **20:** 9–19.

Prince, S., S. Carreira, K. W. Vance, A. Abrahams and C. R. Goding, 2004 Tbx2 directly represses the expression of the p21(WAF1) cyclin-dependent kinase inhibitor. Cancer Res. **64:** 1669–1674.

Rhyu, M. S., and J. A. Knoblich, 1995 Spindle orientation and asymmetric cell fate. Cell **82:** 523–526.

Rhyu, M. S., L. Y. Jan and Y. N. Jan, 1994 Asymmetric distribution of numb protein during division of the sensory organ precursor cell confers distinct fates to daughter cells. Cell **76:** 477–491.

Roy Chowdhuri, S., T. Crum, A. Woollard, S. Aslam and P. G. Okkema, 2006 The T-box factor TBX-2 and the SUMO conjugating enzyme UBC-9 are required for ABa-derived pharyngeal muscle in C. elegans. Dev. Biol. **295:** 664–677.

Shen, C. P., L. Y. Jan and Y. N. Jan, 1997 Miranda is required for the asymmetric localization of Prospero during mitosis in Drosophila. Cell **90:** 449–458.

Smith, P. A., and S. E. Mango, 2007 Role of T-box gene tbx-2 for anterior foregut muscle development in C. elegans. Dev. Biol. **302:** 25–39.

Spana, E. P., C. Kopczynski, C. S. Goodman and C. Q. Doe, 1995 Asymmetric localization of numb autonomously determines sibling neuron identity in the Drosophila CNS. Development **121:** 3489–3494.

Sulston, J. E., E. Schierenberg, J. G. White and J. N. Thomson, 1983 The embryonic cell lineage of the nematode Caenorhabditis elegans. Dev. Biol. **100:** 64–119.

Trent, C., N. Tsuing and H. R. Horvitz, 1983 Egg-laying defective mutants of the nematode *Caenorhabditis elegans*. Genetics **104:** 619–647.

Troemel, E. R., J. H. Chou, N. D. Dwyer, H. A. Colbert and C. I. Bargmann, 1995 Divergent seven transmembrane receptors are candidate chemosensory receptors in C. elegans. Cell **83:** 207–218.

Uemura, T., S. Shepherd, L. Ackerman, L. Y. Jan and Y. N. Jan, 1989 numb, a gene required in determination of cell fate during sensory organ formation in Drosophila embryos. Cell **58:** 349–360.

Wang, B. B., M. M. Muller-Immergluck, J. Austin, N. T. Robinson, A. Chisholm *et al.*, 1993 A homeotic gene cluster patterns the anteroposterior body axis of C. elegans. Cell **74:** 29–42.

White, J. G., E. Southgate, J. N. Thomson and S. Brenner, 1986 The structure of the nervous system of the nematode Caenorhabditis elegans. Philos. Trans. R. Soc. Lond. B Biol. Sci. **314:** 1–340.

Communicating editor: M. Nonet